

This manuscript is the Author's Accepted Manuscript for the following publication:

Árpád Bihari, Zoltán Dezső, Tibor Bujtás, László Manga, András Lencsés, Péter Dombóvári, István Csige, Tibor Ranga, Magdolna Mogyorósi & Mihály Veres (2014) Fission products from the damaged Fukushima reactor observed in Hungary, *Isotopes in Environmental and Health Studies*, 50:1, 94-102, DOI: 10.1080/10256016.2013.828717

Fission products from the damaged Fukushima reactor observed in Hungary

Árpád Bihari^{a,*}, Zoltán Dezső^b, Tibor Bujtás^c, László Manga^c, András Lencsés^c, Péter Dombóvári^c, István Csige^a, Tibor Ranga^c, Magdolna Mogyorósi^a, Mihály Veres^b

^a *Hertelendi Laboratory of Environmental Sciences, Institute of Nuclear Research, Hungarian Academy of Sciences, H-4001, P. O. Box 51, Debrecen, Hungary*

^b *Isotoptech ZRt., H-4001, P.O.Box 360, Debrecen, Hungary*

^c *Paks Nuclear Power Plant Ltd., H-7031, P.O.Box 71, Paks, Hungary*

*Corresponding author E-mail: bihari.arpad@atomki.mta.hu

Tel: +3652509200 /11217

Fax: +3652509208

Fission products from the damaged Fukushima reactor observed in Hungary

Fission products, especially ^{131}I , ^{134}Cs and ^{137}Cs from the damaged Fukushima Dai-ichi Nuclear Power Plant have been detected many places worldwide shortly after the accident caused by natural disaster. To observe the spatial and temporal variation of these isotopes in Hungary, aerosol samples have been collected at five locations from late March to early May 2011: Institute of Nuclear Research, Hungarian Academy of Sciences (ATOMKI, Debrecen, East-Hungary), Paks NPP (Paks, South-Central-Hungary) as well as at the vicinity of Aggtelek (Northeast-Hungary), Tapolca (West-Hungary) and Bataapati (Southwest-Hungary) settlements. In addition to the aerosol samples, dry/wet fallout samples have been collected at ATOMKI, and airborne elemental iodine and organic iodide samples have been collected at Paks NPP. The peak in the activity concentration of airborne ^{131}I has been observed around 30 March (1-3 mBq/m³ both in aerosol samples and gaseous iodine traps) with slow decline afterwards. Aerosol samples of several hundred cubic meters of air showed ^{134}Cs and ^{137}Cs in detectable amounts along with ^{131}I . The decay corrected inventory of ^{131}I fallout at ATOMKI was 2.1 ± 0.1 Bq/m² at maximum in the observation period. Dose-rate contribution calculations show that the radiological impact of this event at Hungarian locations has been of no considerable concern.

Keywords: ^{131}I , ^{134}Cs , ^{137}Cs , Fukushima, aerosol, fallout

1. Introduction

Gaseous (esp. $^{131\text{m}}\text{Xe}$, ^{133}Xe , $^{133\text{m}}\text{Xe}$ and ^{135}Xe) and volatile (especially ^{131}I , ^{132}I , ^{132}Te , ^{134}Cs and ^{137}Cs) fission products from the damaged Fukushima Dai-ichi nuclear power plant have been detected by the International Monitoring System (IMS) of the Comprehensive Nuclear-Test-Ban Treaty Organization shortly after the accident caused by natural disaster [1]. Bowyer et al. [2] and Sinclair et al. [3] reported on the occurrence of radioxenon isotopes on the west coast of USA and Canada, respectively, as early as 16 March 2011, while Diaz Leon et al. [4] and Norman et al. [5] reported on the presence of radioiodine, radiothallium and radiocaesium isotopes in aerosol and rainwater samples,

respectively, on the west coast of USA as early as 18 March. The dispersion of ^{131}I in the air above Europe was first detected at Iceland on 19-20 March, with radiocaesium and radiothallium isotopes following 4 days later [6].

This work reports data on the spatial and temporal variation of ^{131}I , ^{134}Cs and ^{137}Cs in Hungary from 23 March till the first days of May 2011 based on aerosol samples collected at five locations, fallout samples collected at one location and gaseous elemental iodine and organic iodide samples collected at one location. Effective decay constants of ^{131}I and ^{134}Cs as well as isotopic ratios of $^{131}\text{I}/^{137}\text{Cs}$ and $^{134}\text{Cs}/^{137}\text{Cs}$ have been compared with available published data. Dose-rate contribution calculations from airborne isotopes and from fallout have also been performed for adults.

2. Experimental

2.1. Sampling

Aerosol samples have been taken at the following locations (Fig. 1) using glass-fibre filter materials (collection efficiency assumed to be better than 95% for the relevant size-fractions):

- (A) Institute of Nuclear Research of the Hungarian Academy of Sciences (ATOMKI) situated in Debrecen, East-Hungary. Two portable aerosol samplers (12 m³/h air current for shorter operating times, assembled at ATOMKI; 6 m³/h air current for longer operating times, DL-1E, F&J) have been used with glass-fibre filter plates of 0.45 µm mesh and 41 mm effective diameter. Total sample sizes varied between about 15 m³ and 130 m³.
- (B) Monitoring stations situated around Paks NPP (Paks, South-Central-Hungary). On these stations high capacity aerosol samplers (KS-301-APT, Kalman System Ltd., Hungary) with nominal air current of 40 m³/h are operated, collecting on

MN85/90 glass-fibre filter plates of 200 mm diameter. The filter plates have been changed either weekly or 2 times a week.

- (C) Monitoring stations situated around the National L/ILW Radioactive Waste Repository in the vicinity of Bábaapáti settlement (Southwest-Hungary). On these stations CANBERRA iCam Alpha/Beta Air Monitors are operated in which aerosols are collected on 25 mm wide glass-fibre filter tapes with a nominal air current of 2.2 m³/h. Tapes are forwarded typically after 20-30 m³ of air filtered.
- (D) Occasional sampling with a portable high capacity (30 m³/h) aerosol sampler (KS-301-F, Kalman System Ltd., Hungary) operated in the vicinity of Tapolca settlement (West-Hungary), collecting on a glass-fibre filter plates of 150 mm diameter.
- (E) Occasional sampling with a portable aerosol sampler from ATOMKI operated in the vicinity of Aggtelek settlement (North-Hungary).

Dry/wet fallout samples have been collected at ATOMKI with a 0.219 m² dish. Rainwater samples have been concentrated by evaporation onto a stainless steel dish of 50 mm diameter. To avoid any loss of iodine isotopes during heating, the pH of collected water has been set to about 10 with 0.025M NaOH solution. Dry fallout samples have been washed into a glass beaker with 100 ml of 0.025 M NaOH solution containing 5 mmol of KI as carrier, evaporated subsequently onto a stainless steel dish of 50 mm diameter.

At Paks NPP monitoring stations, aerosol samplers also contain elemental iodine and organic iodide traps, sequentially after the aerosol filter plates. These are collecting on silver impregnated activated charcoal filter plates (Kalman System Ltd., Hungary) and on NUCLEARCARB 207B 5TEDA (CHEMVIRON CARBON, Belgium) activated

charcoal filter cartridges, respectively, with the same effective diameter as the aerosol filter.

2.2. Measurement

Gamma-spectrometry measurements have been carried out either at ATOMKI for samples from locations A, C, D and E or at the Environmental Monitoring Laboratory of Paks NPP for samples from location B following standard procedures. Gamma-ray spectrometry systems (ORTEC and CANBERRA) with high purity Ge detector and gamma analysis software have been used. The systems have been calibrated for all the necessary geometries both with a multi-isotope standard (manufacturer: Hungarian Metrological Office, product code: OMH-MIX-11900) and ^{131}I sources (manufacturer: Izinta Ltd., product codes: 99-045 and 99-041). Coincidence corrections for the evaluation of ^{134}Cs gamma peaks have been performed via appropriate software (like the LabSOCS module of CANBERRA) and the Total/Photo calibration of the systems. To ensure good counting efficiency, samples have been placed as close as possible to the detector caps, with larger samples compacted as much as possible before measurement.

All activity data have been decay-corrected in two steps: using the ‘decay during sampling’ model (implementing the well-known differential equation used for the same purpose e.g. in radon studies) of the gamma-spectrometry software to the end of the collection period and then to the median of the collection period using simple decay calculation.

3. Results and discussion

3.1. Distribution of ^{131}I in aerosol samples

Temporal variation of activity concentration of ^{131}I (in $\mu\text{Bq}/\text{m}^3$) in aerosol samples from

all sampling locations is shown in Fig. 2 (1σ uncertainties included). The temporal scope of data points are defined by horizontal error bars.

One can observe the following general picture: there is an ascent in ^{131}I concentration between the beginning of the observation period and a clearly visible primary maximum around 30-31 March. This ascension is of exponential nature (linear at semi-logarithmic scale) which is confirmed by fitting an exponential growth function (see dashed line in Fig. 2). A maximum of $3.5\pm 0.2 \text{ mBq/m}^3$ ^{131}I concentration has been observed at Tapolca sampling site. The descent of ^{131}I concentration after the primary maximum till the first days of May is also of exponential nature. This part of the distribution has been fitted with a first-order exponential decay function (see dotted line in Fig. 2). The effective decay constant of particulate ^{131}I ($\tau_{131,a}$) obtained from the fitting is $0.152\pm 0.002 \text{ d}^{-1}$ (atmospheric removal half life: $6.58\pm 0.07 \text{ d}$) which is well within the range reported by Bossew et al. (Median: 0.167 d^{-1} , 5%-quantile: 0.117 d^{-1} , 95%-quantile: 0.315 d^{-1}) [7,p.24]. Also within the descending part of the distribution, however, there seems to be a less distinct secondary maximum on 6 April (around 1 mBq/m^3 in concentration). The position of primary and (possible) secondary maximum is indicated with arrows in Fig. 2.

In comparison, for Germany, which is northern west of Hungary, the primary and secondary maximum in ^{131}I concentration was on 29 March (more than 2 mBq/m^3) and on 6 April (more than 1 mBq/m^3), respectively [8], showing a roughly 1 day transportation time as well as a similar ^{131}I concentration of the radioactive material. In contrast, in Greece the first maximum has been detected on 26-27 March (around $300 \mu\text{Bq/m}^3$) and the second one 4-5 April (around $500 \mu\text{Bq/m}^3$) [9]. Similar trend (i.e. higher ^{131}I concentration at the second maximum than at the first one) has also been observed at Iceland [6] and Lithuania [10], for example.

As it can be seen, the data points from Paks NPP are longer term (usually 3-8 days) averages with regular sampling, while the data points from other places (especially from ATOMKI) provide information on narrower time intervals (typically 6-18 hours) with less uniform pattern. The former sampling pattern provides lower detection limits and counting uncertainties but is less responsive to changes while the latter is more responsive to changes but usually possess higher detection limits and counting uncertainties. The combination of these two sampling patterns can provide as much information as a uniform daily (e.g. [6]) or 2-days-long sampling (e.g. [9]). Although the average distance between the sampling points is about 200 km, the differences between concentrations detected at the same time for different places are always within a factor of 2.

3.2. Distribution of organic- and elemental-¹³¹I in Paks NPP samples

Temporal variation of ¹³¹I concentration in organic iodide and elemental iodine samples from Paks NPP monitoring stations is shown in Fig. 3 (1 σ counting uncertainties included). As in case of Fig. 2, the temporal scope of data points are defined by horizontal error bars.

These two ¹³¹I forms show similar temporal distributions to that of aerosol ¹³¹I. Although the temporal resolution of available data is too coarse to identify the exact position of the maximum, it assumed to be located near the beginning of the 31 March to 4 April sampling interval in case of both ¹³¹I forms. The most probable position of the maximum is indicated in Fig. 3 with an arrow (31 March). In comparison, Gudelis et al. [10] also reported a maximum concentration in gaseous ¹³¹I form in the sample collected between 29 March and 1 April at Vilnius, Lithuania. As in case of Fig. 2, the distributions have been fitted with exponential growth and decay functions, respectively (see legend in Fig. 3).

The effective decay constants of organic and elemental form ^{131}I obtained from the respective fittings are $\tau_{131,o} = 0.116 \pm 0.002 \text{ d}^{-1}$ (atmospheric removal half life: $8.65 \pm 0.18 \text{ d}$) and $\tau_{131,e} = 0.141 \pm 0.003 \text{ d}^{-1}$ (atmospheric removal half life: $7.08 \pm 0.17 \text{ d}$), respectively. That is, the atmospheric removal of these forms is a bit slower than that of particulate form. A possible explanation to this is that these forms are subjected to dry deposition significantly less than that of aerosol form.

The average ratio of elemental form ^{131}I to aerosol form ^{131}I and of organic form ^{131}I to aerosol form ^{131}I has been 0.6:1 and 2.4:1, respectively. That is, the aerosol-associated ^{131}I concentration makes up about 25% of the total ^{131}I activity which is also in good correlation with the findings of both Gudelis et al. [10] and Bossew et al. [7], for example. Since the data from Paks NPP in case of aerosol form ^{131}I did fit well into the Hungarian average, the same is assumed to be valid for these ^{131}I forms as well.

3.3. $^{131}\text{I}/^{137}\text{Cs}$ and $^{134}\text{Cs}/^{137}\text{Cs}$ isotope ratios in aerosol samples

Radiocaesium isotopes have been detected since 29 March in aerosol samples with acceptable certainty. The temporal variations of $^{131}\text{I}/^{137}\text{Cs}$ and $^{134}\text{Cs}/^{137}\text{Cs}$ activity concentration ratios are shown in Fig. 4 (data from Tapolca and Paks NPP locations). These ratios have been fitted with Eq. (1) (see also [4])

$$r(t) = r_0 e^{-t(\tau_x - \tau_{137,a})} \quad (1)$$

where $\tau_{137,a}$ is the effective decay constant for particulate ^{137}Cs , while τ_x is either $\tau_{131,a}$ (for particulate ^{131}I) or $\tau_{134,a}$ (for particulate ^{134}Cs), depending on the ratio in question.

From the fitting of the $^{131}\text{I}/^{137}\text{Cs}$ ratio (see dashed line in Fig. 4), using the previously determined $\tau_{131,a}$ value, we obtained a $\tau_{137,a}$ value of $0.086 \pm 0.003 \text{ d}^{-1}$ (atmospheric removal half life: $11.60 \pm 0.44 \text{ d}$). With the obtained $\tau_{137,a}$ value, the temporal

distribution of the $^{134}\text{Cs}/^{137}\text{Cs}$ ratios has also been fitted (see dotted line in Fig. 4). As it can be seen, the $^{134}\text{Cs}/^{137}\text{Cs}$ activity ratio was fairly constant, with an r_0 value of 0.85 ± 0.04 . The obtained $\tau_{134,a}$ value is practically the same as that of $\tau_{137,a}$ and it also well within the range reported by Bossew et al. (Median: 0.099 d^{-1} , 5%-quantile: 0.061 d^{-1} , 95%-quantile: 0.321 d^{-1}) [7,p. 24]. These findings are in good agreement with the observations of other parties (e.g. [4], [6], [9]) as well.

3.4. Dry, wet and mixed fallout of ^{131}I at ATOMKI

The temporal variation of the deposition density of ^{131}I fallout (mBq/m^2) at ATOMKI is shown in Fig. 5. For dry and mixed fallout samples, the temporal scopes of the data points are defined by horizontal error bars. (The duration of rainfall events has been much shorter than the collection periods of dry fallout samples and thus they are not presented.) By mixed fallout sample we understand that the dry fallout sample of a given period had not been collected before the next rainfall event occurred. That is, more or less wet fallout was mixed to these samples.

As one can expect, the flux density of dry fallout samples have been at least one order of magnitude lower than that of wet ones. For dry fallout, with the assumption that only the aerosol form ^{131}I was subjected to deposition, and with deposition velocity defined as the quotient of flux density (in $\mu\text{Bq}/\text{m}^2\cdot\text{d}$) and of concentration (in $\mu\text{Bq}/\text{m}^3$) the average daily dry deposition velocity has been calculated as shown in Table 1, based on the three purely dry fallout samples. The weighted average of dry deposition velocity is $107\pm 34\text{ m}/\text{d}$. With this data, we have been able to calculate the daily flux densities of dry deposition for periods without sampling (i.e. 23-27 March and 18-30 April).

The decay corrected estimated inventory of ^{131}I fallout (also in mBq/m^2) is also presented in Fig. 5 (solid line, second y-axis). The inventory reached its peak around 13 April ($2.1\pm 0.1\text{ Bq}/\text{m}^2$) due to several rainfall events between 12 April and 15 April and

is estimated to decrease to a negligible level within 3 weeks after the observation period. Neither ^{134}Cs nor ^{137}Cs have been detected in the fallout samples at detection limits of about 40-50 mBq/m².

3.5. Dose-rate contribution calculations

Based on the data presented in the previous sections, average Hungarian effective dose-rate contributions (immersion + committed via inhalation) from airborne isotopes (^{131}I , ^{134}Cs and ^{137}Cs) have been estimated for adults. No shielding factor (see [11]) has been applied and 1 m³/h respiration rate has been assumed. Committed effective dose per unit intake via inhalation factors for age group >17 a have been taken from IAEA Safety Series No. 115 [12]. Results are summarized in Table 2. As one can observe, the contribution from the inhalation of organic ^{131}I is the most prominent, due to its increased biological effectiveness and highest concentration among the three ^{131}I forms studied.

Additionally, a location-specific effective external dose-rate contribution from ^{131}I fallout at ATOMKI has been calculated for adults, assuming 1 m distance from soil surface (data taken from Fig. 5). The contribution from this source is estimated to have been about 0.02 nSv/10% outdoor time for the observation period. That is, it has been only 1% of the previous sources at maximum.

4. Conclusions

Due to the large distance between source and deposition area, only traces of the emissions from Fukushima were detectable in Hungary. Dose contribution from airborne and fallout isotopes is estimated to be 18 nSv for adult population at maximum for the observation period (6 weeks). In comparison, dose contribution in the vicinity of Paks NPP from its normal operation is about 45 nSv/year, i.e. 5 nSv for the same 6-week period. Consequently, the radiological impact of this event at Hungarian locations has been of no

considerable concern.

Acknowledgements

We would like to acknowledge 1) the samples from sampling location C (Bátaapáti) to the Public Limited Company for Radioactive Waste Management (PURAM), 2) the samples from sampling location D (Tapolca) to Stieber Environmental Protection Ltd., and 3) the loan of equipment (aerosol samplers and ORTEC HPGe gamma spectrometer) to the Dept. of Environmental Physics of Debrecen University/ATOMKI.

References

1. CTBTO [Internet]. CTBTO Preparatory Commission, Fukushima-related Measurements by CTBTO; 2011. Available from: <http://www.ctbto.org/press-centre/highlights/2011/fukushima-related-measurements-by-the-ctbto/fukushima-related-measurements-by-the-ctbto-page-1/>
2. Bowyer T, Biegalski SR, Cooper M, Eslinger PW, Haas D, Hayes JC, Miley HS, Strom DJ, Woods V. Elevated radioxenon detected remotely following the Fukushima nuclear accident. *J. Environ. Radioa.* 2011;102:681-687.
3. Sinclair LE, Seywerd HCJ, Fortin R, Carson JM, Saull PRB, Coyle MJ, Van Brabant RA, Buckle JL, Desjardins SM, Hall RM. Aerial measurement of radioxenon concentration off the west coast of Vancouver Island following the Fukushima reactor accident. *J. Environ. Radioa.* 2011;102:1018-1023.
4. Diaz Leon J, Jaffe DA, Kaspar J, Knecht A, Miller ML, Robertson RGH, Schubert AG. Arrival time and magnitude of airborne fission products from the Fukushima, Japan, reactor incident as measured in Seattle, WA, USA. *J. Environ. Radioa.* 2011;102:1032-1038.
5. Norman EB, Angell CT, Chodash PA. Observations of Fallout from the Fukushima Reactor Accident in San Francisco Bay Area Rainwater. *PLoS ONE* 2011;6(9):e24330. doi:10.1371/journal.pone.0024330
6. IRSA [Internet]. Icelandic Radiation Safety Authority, Summary of Radionuclide Concentrations in Air, March 19th - April 13th, Reykjavík, Iceland; 2011. Available from: http://www.gr.is/media/skyrslur/Iceland_aerosol_conc_2011_04_15.pdf

7. Bossew P, Kirchner G, De Cort M, de Vries G, Nishev A, de Felice L. Radioactivity from Fukushima Dai-ichi in air over Europe; part 1: spatio-temporal analysis. *J. Environ. Radioa.* 2012;114:22-34.
8. Pittauerová D, Hettwig B, Fischer HW. Fukushima fallout in Northwest German environmental media. *J. Environ. Radioa.* 2011;102:877-880.
9. Manolpoulou M, Vagena E, Stoulos S, Ioannidou A, Papastefanou C. Radioiodine and radiocesium in Thessaloniki, Northern Greece due to the Fukushima nuclear accident. *J. Environ. Radioa.* 2011;102:796-797.
10. Gudelis A, Druteikiene R, Lujaniene G, Maceika E, Plukis A, Remeikis V. Radionuclides in the ground-level atmosphere in Vilnius, Lithuania, in March 2011, detected by gamma-ray spectrometry. *J. Environ. Radioa.* 2012;109:13-18.
11. UNSCEAR. Sources and Effects of Ionizing Radiation, UNSCEAR 2008 Report to the General Assembly with Scientific Annexes, Volume I, Annex B; 2008.
12. IAEA. International Basic Safety Standards for Protection against Ionizing Radiation and for the Safety of Radiation Sources, IAEA Safety Series No. 115; 1996.

Table 1. Calculation of the dry deposition velocity of aerosol form ^{131}I .

Date and duration of collection	Deposition density ($\mu\text{Bq}/\text{m}^2$)*	Flux density ($\mu\text{Bq}/\text{m}^2 \cdot \text{d}$)*	Average ^{131}I activity concentration, aerosol form ($\mu\text{Bq}/\text{m}^3$)*	Deposition velocity (m/d)*
28/3 – 01/4, 4.2 d	326000±41000	77600±9800	910±447	85.3±43.3
01/4 – 04/4, 2.6 d	81000±36000	31200±13900	575±359	54.3±41.6
15/4 – 18/4, 3.0 d	60000±37000	20000±12300	114±18	176±112

* All activities decay corrected to median of the respective collection period

Table 2. Summary of effective dose contributions from ^{131}I , ^{134}Cs and ^{137}Cs in the observation period (Hungarian average, for adults).

Source	Effective dose [nSv/period]					
		^{131}I		^{134}Cs	^{137}Cs	Total
Immersion		0.078±0.003		0.006±0.001	0.003±0.001	0.086±0.002
Committed via inhalation	2.31±0.06 ^a	4.14±0.19 ^e	11.3±0.3 ^o	0.15±0.01 ^a	0.12±0.01 ^a	18.0±0.4
Generic sum		17.8±0.4		0.16±0.01	0.12±0.01	18.1±0.4

^a Aerosol form

^e Elemental form

^o Organic form

Figure 1. Map of Hungary with the position of the sampling locations (see text for details)



Figure 2. Temporal variation of ^{131}I concentration in aerosol samples in Hungary

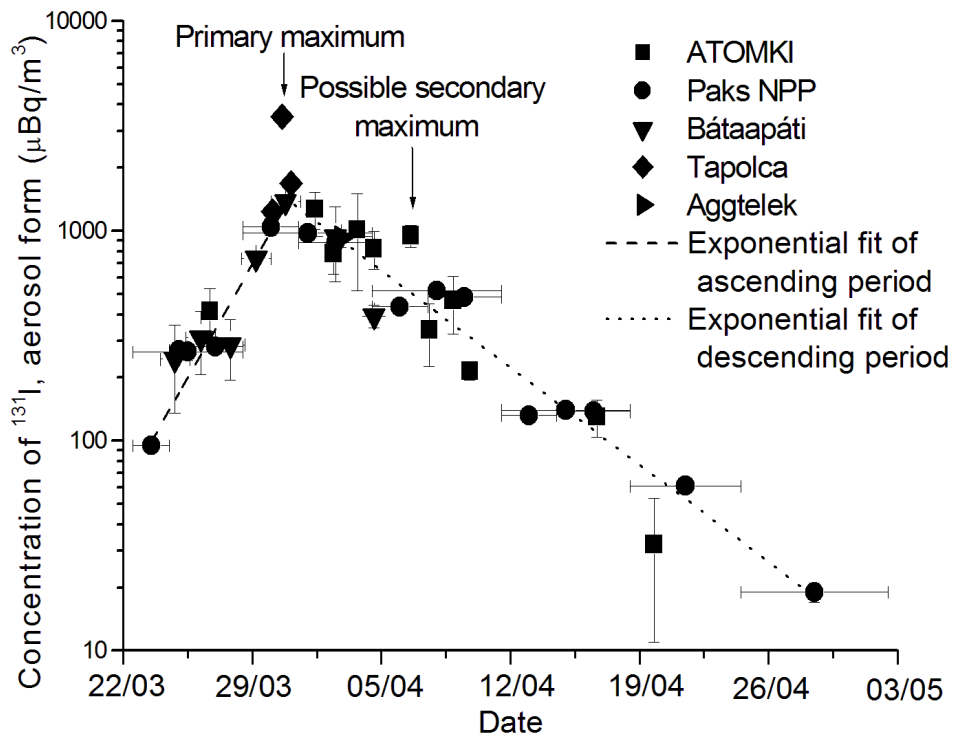


Figure 3. Temporal variation of ^{131}I concentration in elemental iodide and organic iodine samples at Paks NPP

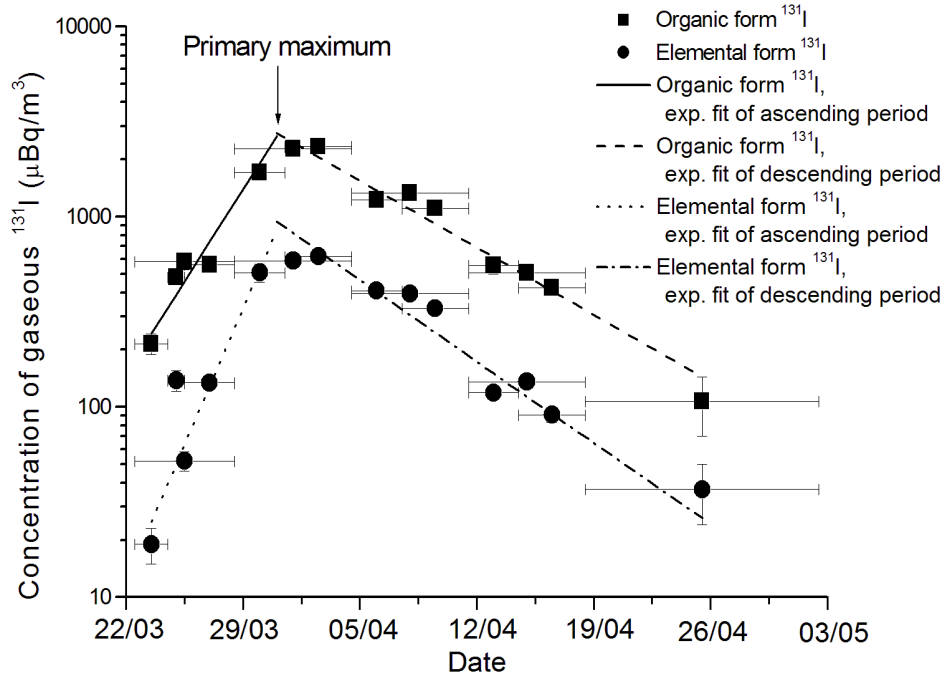


Figure 4. Temporal variations of isotopic ratios in aerosol samples

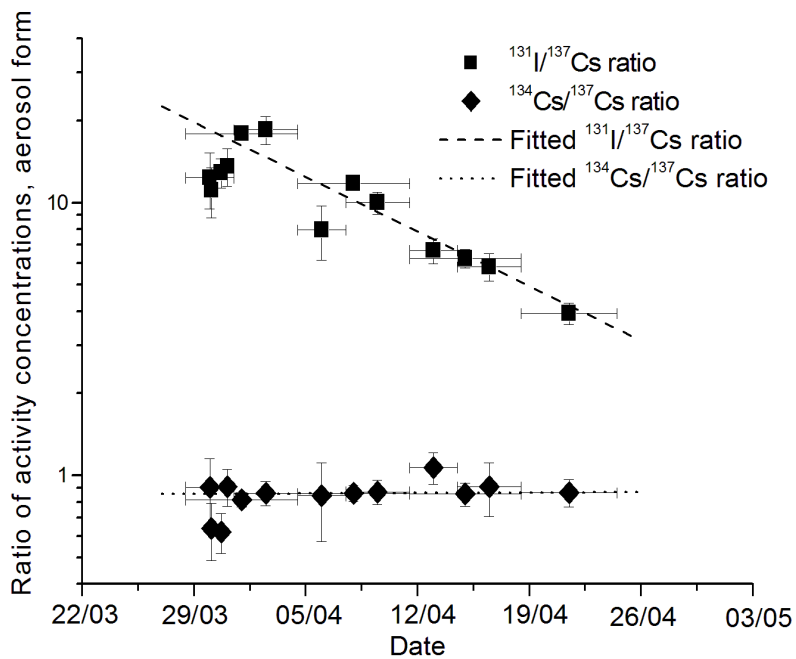


Figure 5. Temporal variation of ^{131}I deposition density of dry, wet and mixed fallout samples at ATOMKI

